

Structure and evolution of Upheaval Dome: A pinched-off salt diapir

M. P. A. Jackson, D. D. Schultz-Ela, M. R. Hudec, I. A. Watson, M. L. Porter:

PART 1. FIELD MAPPING AND METHODOLOGY

Access to most of Upheaval Dome is only possible on foot. Barriers are created by the precipitous Wingate cliffs enclosing the inner depression (Fig. 3) and the outer rim of the mesa surrounding the dome. Conventional access to the central depression is by the circular Syncline Loop trail, then through the portal of Upheaval Canyon. Instead, we directly descended the eastern inner cliff.

Erosional alcoves in the outer margin of Upheaval Dome were reached by foot from Upheaval Bottom in the west, from Trail Canyon in the east, or from the White Rim road in the south.

The whole of the dome was geologically mapped in 1991–1992 at a scale of 1:10,000 (Fig. 6) using conventional field methods augmented by stereoscopic interpretation of monochrome aerial photographs and a false-color Landsat TM image. The panoramas are tracings of slides that were interpreted in the office based on field sketches and notes. The more complex panoramas were re-checked during the second field season. The inner depression was mapped on the ground at a scale of 1:4,000 (Fig. 7), aided by color prints photographed from many vantage points on the encircling cliffs.

The structure contour map (Fig. 2) had two data sources. We surveyed Wingate thicknesses and elevations of its base in Upheaval Dome area using the following combination of optical instruments: bearing compass, self-damping clinometer, and range finders designed for distances up to 200 m and 1000 m. Elevations for the surrounding area were taken from the map by Huntoon et al. (1982).

PART 2: VOLUMETRIC CALCULATIONS

Deviation of rock volumes from typical regional values just outside Upheaval Dome elucidates its evolution. The deviations constrain primary (sedimentary) thickness variations, structural effects, and salt loss. Here we describe two types of calculations: (1) variation in elevation of a horizon relative to its regional trend, and (2) variation in thickness of a layer. The first calculation was fully three dimensional. In the second calculation, data were limited, so we extrapolated thickness variations from a well-exposed cross section by assuming the structure was symmetric about a central axis. We assumed that horizons were deposited at the extrapolation of their regional datum surface; that is, relief was negligible except for any emergent salt domes.

The results indicate substantial cumulative loss of salt from the system and sedimentary thickening adjoining the dome during deposition of at least the Chinle Formation.

Volume Imbalance at Base Wingate

The impact hypotheses allow for some lateral flow of Paradox salt but entail no overall loss of salt volume because the salt was not exposed to dissolution. Thus, the volume (W_{C+}) of rock raised above this regional datum by later contraction in the inner dome is equal to the volume (W_{e-}) depressed below regional datum by extension in the dome periphery.

$$W_{C+} = W_{e-} \quad (1)$$

Conversely, the pinch-off hypothesis requires massive loss of salt as the overhanging, formerly extrusive lobe of salt dissolved. Moreover, the simple volume balance of contraction versus extension (Equation 1) is complicated by the additional effects of salt dissolution (W_{d+}) versus salt withdrawal (W_{w-}) as follows:

$$W_{c+} + W_{d+} = W_{e-} + W_{w-}, \quad (2)$$

where the left side represents the volume of rock emplaced above regional datum, and the right side represents the volume of rock depressed below regional datum. The salt dissolved (W_{d+}) in the pinch-off hypothesis would have vanished, but its volume should be calculable by rearranging Equation 2 as

$$W_{d+} = (W_{-}) - (W_{c+}), \quad (3)$$

where W_{-} is the volume of rock depressed below regional datum by a combination of extension and salt withdrawal. Because W_{d+} was lost by dissolution, the pinch-off hypothesis predicts a gross volume imbalance: the subsided volume should be more than the uplifted volume.

The two hypotheses are thus testable by volume balance. The structure contour map on the base of the Wingate (Fig. 2) provides the most reliable volumetrics because the horizon is well exposed and unambiguously identifiable both in the Upheaval Dome structure and in the region beyond.

Commercial software, CPS-3, was used to calculate the volumetric deviations at Upheaval Dome. The contoured map area was gridded to 25-m squares to form a smoothed three-dimensional surface. Contours projected across the Upheaval Dome geometric perturbations defined the regional homoclinal trend surface. The volumes of contour deviations above and below the regional trend were then calculated separately to find W_{C+} and W_- as defined above (Fig. A1). The lack of Wingate outcrop in the center of the dome created minor variation in the calculated volume above regional. Two bounding cases were considered. First, the base Wingate horizon was projected straight across the dome center at the height of its innermost outcrop; that gave a minimum possible W_{C+} (solid contours in Fig. A1). Second, the Wingate horizon was projected to the center of the structure (dashed contours in Fig. A1) parallel to the underlying preserved Moenkopi to form a vertically stretched cone; that gave a probable maximum for W_{C+} .

The total volume displaced by peripheral depression of the base Wingate horizon below regional datum (an area of 18.5 km²) is 0.74 km³. Conversely, the volume emplaced by central uplift of the Wingate horizon (an area of 5.3 km²) ranges from 0.29 to 0.34 km³. Because of their small circumference, changes in the central contours have little effect on the overall volumes. Even for a stretched cone of vanished Wingate in the dome's core, an assumption that favors the impact hypothesis, W_- exceeds W_{C+} by a factor of more than 2 to 1. This gross imbalance suggests (by Equation 3) that at least 0.4 km³ of rim syncline volume beneath the Wingate has been lost from Upheaval Dome. There is no evidence for thickening of the Paradox salt immediately outside the dome. Thus, loss of salt through diapiric expulsion and dissolution is the only reasonable process for this magnitude of volume loss. These processes are incompatible with the impact hypotheses.

Volume Variation of Chinle Formation

The above calculations indicate the volume of salt lost from the system since deposition of basal Wingate strata. Data for an additional horizon allow calculation of salt lost during the time period separating the two horizons. Exposures of other contacts are not sufficiently continuous throughout the structure to accurately map a three-dimensional surface. However, in two dimensions, the basal Chinle contact (marked by the prominent Mossback conglomerate) is exposed or readily inferred from the center of the dome through Upheaval Canyon to beyond the rim monocline (Fig. 9). To calculate the area of the Chinle Formation, we used the base Wingate and base Chinle contacts in the northwest half of the cross section of Figure 9 as a representative slice of the Chinle. The volume of the Chinle was estimated by assuming symmetry about the center of the structure; that assumption is validated below. The central axis of the dome lies at the apex of the Cutler contact on the cross section. The Chinle contacts were projected from their innermost outcrop on the cross section to the center parallel to the underlying Cutler contact. As for the preceding section, the form of the inward extrapolation has little influence on the volumetrics.

To simplify calculations, the upper and lower Chinle contacts were rotated 1.8° to remove the regional dip to the northwest. Our coordinate system had the horizontal axis increasing outward from the center of the dome and zero elevation at the regional Chinle base (Fig. A2a). This system places the regional Chinle-Wingate contact at 0.1 km elevation. Elevations measured from the section at horizontal 0.1-km intervals defined the contacts, which were then approximated by smooth curves calculated using: (1) best-fit 8th-order polynomials, and (2) cubic spline interpolations between the control points (Fig. A2a). Exact volumes were integrated from the polynomials using the method of

cylindrical shells. In addition, approximate volumes were summed from shells bounded by linear interpolations between spline points 0.01 km apart. Results of the two types of volume calculations differed by less than 2%.

First, consider the top Chinle (basal Wingate) contact. Figure A2a shows elevations of this contact above and below the regional elevation (0.1 km). Revolving the contact about the center should define a volume similar to that calculated from the map (Fig. A1) if the structure were truly symmetric. The area above regional sweeps a volume W_{C+} defined above, and the area below regional sweeps a volume W_- . Based on the cubic spline interpolation, the volumetric deviation, W_{d+} (vanished salt), from regional is -0.37 km^3 as compared with -0.41 km^3 for the full three-dimensional calculation above. Thus, the structure appears to deviate only $\sim 10\%$ from axial symmetry, and the line of section is representative.

Second, the difference between the upper and lower Chile contacts can be compared with the regional thickness of 0.1 km to assess thickness variations. Figure A2b shows thickness variation relative to a flattened regional top Chinle contact. Parts of the layer thinner and thicker than regional lie above and below the regional thickness of 0.1 km. The Chinle Formation inward from the monocline thickens and thins slightly, then thickens substantially from a distance of 1.49 km to the dome center. The calculated volume of the Chinle layer from the monocline to the center is 2.45 km^3 , denoted C . A tabular regional layer of the same area would contain 2.12 km^3 , denoted C_{tab} . Thus, because of inward thickening, the present volume exceeds that of a layer of regional thickness with the same map area by 0.33 km^3 , denoted C .

The calculated thickening of the Chinle, C , may be the result of primary thickness variations (C_p for volumes of depositional thickening or thinning) or later deformation (C_s for volumes of structural thickening or thinning). Because

no deformation is found outside of the rim monocline, we treat the monocline as fixed through time and consider several cases for initial configuration and changes inward of the monocline. First we consider: *Case 1*: an originally continuous, tabular Chinle layer (C_{tab}) with no central diapir, and therefore no pinch-off, as required by the impact model; and *Case 2*: a Chinle layer that accumulated around a growing diapir that later pinched off. Additional cases vary the relative contributions of initial thickness, primary effects, and structural effects in Case 2.

Case 1 (Fig. A3):

For impact without a central diapir, volume would be approximately conserved in the Chinle layer during deformation, that is, $C_s = 0$. Thus, the observed excess volume must be attributed to primary thickening, which cannot be explained by the impact hypotheses. Conversely, primary thickening near a diapir is a common result of underlying syndepositional salt withdrawal. The net volume change, C , is the present thickness minus the regional thickness of a tabular layer. C is the result of primary and structural changes. But because deformation only redistributes volume, but does not change it,

$$C = 0.33 \text{ km}^3 = C_p + C_s = C_p \quad (4)$$

This net Chinle thickening corresponds to the volume of underlying salt that left the system during Chinle time. For an axisymmetric structure surrounded by virtually undeformed rock, the salt loss can only be plausibly ascribed to flow up the diapir. Thus, because it lacks a diapir, Case 1 is self-contradictory and invalid.

Case 2 (Fig. A3):

If we assume a central diapir during Chinle deposition, the volume of rock inside the rim monocline at that time must have been the sum of (1) the diapir volume between the elevation of the upper and lower Chinle contacts (C_d) and (2) the present Chinle volume ($C = C + C_{tab}$). The diapir volume was later lost to the surface during pinch-off. Thus, the excess Chinle volume relative to an equivalent layer of regional thickness would be even greater than the calculated value of 0.33 km^3 . The larger excess Chinle volume would indicate even more expulsion and dissolution of salt during Chinle deposition.

What about thickness changes caused by pinch-off? The earliest evidence for the onset of pinch-off is the growth folds in the basal Wingate. However, we cannot exclude the possibility that pinch-off could have begun in Chinle time. First, assume that pinch-off began in Wingate time. Then pinch-off is post-depositional and entirely structural with respect to the Chinle. If we can identify the strain contribution to thickness variation, we can calculate an average radius of the diapir during Chinle time. Therefore, we must resolve the overall thickness variations into depositional and deformational components; that is, into C_p and C_s .

Consider variations in the outer part of Upheaval Dome. No evidence for structural thickening (contraction) exists there. Thus, the zones of slight thickening at about 2 and 2.4 km from the center in Figure A2b must be primary variations. These zones probably thinned structurally, because normal faults have been mapped in the Wingate in this section between 1.4 and at least 2.2 km from the center. Thus, the present thickness represents only a minimum possible original thickness in those thicker zones. A reasonable estimate for an original thickness in the outer Chinle is therefore a line projected inward and slightly downward from regional at the rim monocline to the thickest zone at 2.4

km, then continued inward at the same elevation (-0.01 km) to its intersection with the thickening zone in the inner part of the dome at about 1.4 km. A dash-dot line on Figure A2b shows this inferred Chinle thickness, which is also shown in Figure A3 as the "Local reference thickness" (LRT). Diapiric pinch-off would require radial extension as rock moved inward and would therefore vertically thin the Chinle. In the thinned outer part of Upheaval Dome, the net volume deficit is a sum of (1) any unrecognized primary thinning, (2) structural thinning balanced by structural thickening farther inward due to gravity gliding during pinch-off, and (3) structural thinning balanced by inward movement of the necking diapir. The maximum possible diapir diameter during Chinle time can be found by assuming that structural thinning balanced by diapiric necking caused *all* of the outer volume deficit relative to the local reference thickness. If so, the loss of volume relative to the local reference thickness (-0.15 km³) equals the volume of the diapir pinched off, or $C_s = C_d$. The Chinle contacts on Figure A2a indicate a thickness of 0.18 km at the center. Using this thickness for the diapir implies a diapir diameter of 1.0 km.

This inferred diameter assumes that the local reference thickness was modified only by outer structural effects and inner primary effects. Different combinations of reference state, timing, and structural and primary variations change the estimated diapir diameter. Because the available data cannot completely quantify these variations, for most additional cases we will simply indicate the sense of change relative to Case 2.

Case 3 (Fig. A3):

If pinch-off began during Chinle time, the depression caused by structural thinning in the outer part would likely trap extra sediment. Such counteracting primary thickening would necessitate more structural thinning than in Case 2 to

reach the present state. Thus, the inferred diapir diameter would exceed that calculated for Case 2.

Case 4 (Fig. A3):

Conversely to Case 3, any primary thinning relative to the local reference thickness would decrease the calculated structural thinning and thus decrease the calculated diapir diameter in Case 2. However, primary thinning would be unlikely to accompany structural thinning (see Case 3).

Case 5 (Fig. A3):

Consider the extreme case that the primary thickness in the outer part followed the regional thickness, rather than the local reference thickness. Assuming (as in Case 2) only outer structural effects and inner primary effects, the outer thickened bulges imply structural thickening (unrecognized in the field) as well as thinning. But even for this case, the net volume change is still negative (-0.018 km^3), which indicates a diapir diameter of 0.35 km.

Case 6 (Fig. A3):

The preceding analyses assume that all of the observed thickening in the inner part of the dome was primary. Any structural thickening there would partially compensate structural thinning in the outer part and therefore decrease the calculated diapir radius. However, given the large diameter inherent in Case 2, a diapir of more reasonable size, such as shown in the restoration of Figure 26, would allow substantial structural thickening of the inner part.

Summary of Chinle thickness variations

Volumetrics of the Chinle indicate substantial primary thickening, which requires synsedimentary evacuation of underlying salt through a diapir. That is incompatible with impact. Thickness variations in the Chinle have been analyzed in six hypothetical cases combining primary and structural effects. Cases 1 and 4 either use unsupported assumptions or entail conclusions that contradict the

evidence. The most realistic combinations are Case 3 for the outer part of the dome and Case 6 for the inner part. Case 3 predicts a diapir diameter larger than the 1.0 km found for Case 2, and Case 6 predicts a smaller one. The observations cannot determine the exact contributions of these competing effects. However, the data clearly support: (1) a substantial diapir during Chinle time; and (2) syndepositional evacuation of underlying salt and partial pinch-off of the diapir.

FIGURE CAPTIONS

Figure A1: Structure contours showing deflection of the base Wingate horizon above (stippled area) and below (unpatterned) the regional homocline. Contour interval here is 100 ft (30.5 m) but was actually 20 ft (6.6 m) for the volume calculations. The outermost 0-ft contour is equivalent to the rim monocline in Figure 2. The two dashed contours in the dome center define a hypothetical conical shape as one end member for the volumetric calculations.

Figure A2: Vertically exaggerated profiles of the top and bottom of the Chinle Formation, showing various volumetric parameters. The profiles are taken from the northwest leg of the cross section in Figure 9.

Figure A3: Schematic cross sections of the Chinle Formation from the dome center (right end of sections) outward to the northwest (not to scale). Each case has different combinations of primary and structural thinning and thickening and reference state, but each leads to the same present state. See Figure A2 and text for further explanation.

PART 3: EVALUATION OF EVIDENCE FOR PINCH-OFF VERSUS IMPACT

This evaluation is summarized in Table 1 (text). Figure references are to the text figures except for Figures A4 and A5, shown here.

Positive Evidence Compatible With Both Pinch-Off and Impact

Circularity

Upheaval Dome is highly circular, as evident in the circumferential traces of its rim monocline, rim syncline, and central dome (Figs. 2, 8). Impact structures and salt domes both vary in shape from circular to elliptical. Many impact structures, especially those in crystalline basement, were discovered because their circular shape attracted detailed investigation. However, a few suspected impact structures are strongly elliptical because of oblique impact or superposed orogenic shortening. Most salt domes are more elliptical than truly circular, but many circular, overhanging salt stocks are known.

Central Uplift

Bowl-shaped transient impact craters wider than 2–4 km on Earth collapse under gravity to form complex craters (Melosh, 1989). The walls slump inward and, possibly aided by elastic rebound of the floor, create a central peak by arching and faulting of strata above the regional level of equivalent strata. Comparative morphometry for structural uplift versus terrestrial crater diameter translates into a central uplift of 890 m ($= 0.086D^{1.03}$, where D is the diameter of the complex crater; Grieve and Pilkington, 1996) for an impact crater 8.5 km wide (inferred by Shoemaker and Herkenhoff, 1984). For the crater diameters of 6.4 km and 2 km inferred by Kriens et al. (1997), the equivalent central uplifts would be 540 m and 160 m, respectively. Clearly, the wide range of estimated crater diameters for

Upheaval Dome allow an equally wide range of central uplifts. An uplift of 120–250 m is actually present in the core of Upheaval Dome.

A central uplift is also characteristic of pinched-off diapirs imaged by reflection seismic data (Fig. 22). Reflectors indicate festoons of deformed strata, whose outward dip increases inward toward the axial weld representing the pinched-off stem. We ascribe the central mound to constrictional structural thickening related to gravity-driven inward motion during diapiric pinch-off.

Clastic Dikes

Sedimentary dikes record the injection of overpressured, liquified sediment into less-permeable, dilating country rocks. Severe transient overpressuring and injection of clastic dikes are likely in water-bearing sediments near an explosive crater (whether caused by nuclear explosion or meteoritic impact).

On the other hand, clastic dikes produced by non-impact processes are extremely common in the geologic record wherever water-saturated sediments are loaded during burial. Clastic dikes occur in a range of depositional settings from deep-water turbidites to subaerial mass-flow deposits (Collinson, 1994) and form by differential sediment loading, pulses of sedimentation, or seismic events. Some of these settings are dominated by salt tectonics. For example, small sandstone dikes have been reported from the boundaries of collapse structures formed by dissolution of the Moab salt anticline north of Upheaval Dome (Puffett et al., 1957).

In the core of Upheaval Dome, the clastic dikes, probably injected upward from the White Rim, commonly terminate laterally in faults. We infer that the dikes were emplaced along fractures or faults dilated by fluid pressure in strata overpressured by an upper seal of impermeable salt. Such overpressuring is a common engineering challenge to subsalt drilling in the Gulf of Mexico.

Overpressuring would have begun before pinch-off started. Thus, at least some dikes could have been deformed and rotated by axial shearing during pinch-off.

Crushed Quartz Grains

Quartz grains that have been crushed or shattered into pieces in the clastic dikes were used as evidence for impact by Shoemaker and Herkenhoff (1984). We found microfractured quartz in the dikes (Fig. A4). However, even widespread microfractured quartz is geologically common. For example, quartz grains are crushed and mechanically rearranged by compaction during burial (Milliken, 1994; Dickinson and Milliken, 1995); they are common in fault zones within 100 m of even small-displacement (~100 m) fault surfaces (Anders and Wiltschko, 1994). Microfractures are typically masked by recementation of authigenic quartz between and in optical continuity with the shards. Electron beam-induced cathodoluminescence of our Upheaval Dome sample reveals that the quartz undulatory extinction is caused by slightly misoriented grain fragments separated by microfractures sealed with cement. Again, brittle deformation and sealing of this type is common in fault rocks (Anders and Wiltschko, 1994).

Inner Constrictional Zone

An inner constrictional zone with vertical extension implies that rock moved radially inward and was crowded into an increasingly smaller plan area. During constriction, horizontal strata shorten both radially and circumferentially by thrusting, folding, and ductile vertical thickening. Radial shortening creates circumferentially trending folds or thrust faults. Circumferential shortening creates thrust faults with radially trending traces or folds that plunge radially outward. Radial thrust faults represent a brittle response of the inner constriction. Subradial faults occur in parts of many impact structures, such as Goyder (Haines, 1996) and Gosses Bluff (Milton et al., 1996) in Australia. Outward-

plunging folds have been reported in some impact craters (e.g., at Hico, Texas; Milton, 1987).

Similar folding is more difficult to find in pinched-off diapirs. Natural examples are rare because seismic imaging is degraded by the presence of overlying salt. A rare exposure of diapirs whose stems have reached advanced—but incomplete—pinch-off is in the Great Kavir of central Iran. Erosion planed off more than 50 Kavir salt diapirs at different structural levels (Jackson et al., 1990). Upper levels show distended, spreading bulbs, whereas lower levels show the radially folded, tightly constricted stems of almost pinched-off salt diapirs (Fig. A5).

Outer Extensional Zone

The well-developed extensional faults rimming Upheaval Dome (Figs. 14, 17, and 18) dominate the outer structure. Extension typically concentrates near the outer margin of the peripheral sink of salt domes, like fabric stretching and tearing over the rim of a bowl. This extensional rim can correspond to the crest of flanking turtle structures, such as that surrounding Hainesville Dome, East Texas (Jackson, 1982). Extension is also common in large impact craters, where the walls of the transient cavity slump inward during rise of the central peak (Shoemaker and Herkenhoff, 1984). The existence of extension per se cannot differentiate between pinch-off and impact. However, the style of that extension seems more plausible for pinch-off than for impact (see “Lack of Outer Fault Terracing” and “Outward-Verging Extension” below).

Radial Lobes (Dog Tongues)

The dog tongues in Wingate strata rimming the inner depression are unusual structures. At first glance, they seem to have no obvious counterparts in either salt tectonics or impact cratering. Kriens et al. (1997) interpreted these lobes as partly fluidized sandstone that slumped down the walls of the inferred transient

impact crater. Particularly difficult to explain are the lobes' apparent disconformity with underlying strata, their folding on both radial and circumferential axes, their missing stratigraphic section at the base of the lobe, and radial shortening in their outer margin. These complexities are explicable by salt welding (Jackson and Cramez, 1989) where two volumes of rock originally separated by salt are juxtaposed by removal of salt by flow or dissolution (Fig. 19).

Underlying Salt

The indisputable presence of underlying salt is necessary for the pinch-off hypothesis but is not diagnostic of either hypothesis.

Gravity and Magnetic Anomalies

Magnetic and gravity highs centered on Upheaval Dome were reported by Joesting and Plouff (1958). Shoemaker and Herkenhoff (1984) considered these anomalies to support the notion of meteoritic impact. Yet most terrestrial impact structures are characterized by overall gravity and magnetic lows because of fracturing and brecciation (Grieve and Pilkington, 1996). When the map of total magnetic intensity is reprocessed to correct all anomalies to the pole, the prominent magnetic high shifts 2.7 km to the north-northeast and is no longer centered on Upheaval Dome. Moreover, the ~10-km wavelength of this anomaly indicates that it is sourced from within crystalline basement.

Joesting and Plouff (1958) also reported two long-wavelength (9 km) gravity highs in the area. One is on the southern rim of Upheaval Dome, the other on nearby Grays Pasture to the southeast, where there is no evidence for doming. Both anomalies have been ascribed to the influence of locally dense, magnetic basement, probably involving igneous rocks (Joesting and Plouff, 1958). Joesting and Plouff (1958) also showed a small (1.5-km wavelength) positive Bouguer anomaly over the center of Upheaval Dome. However, this

anomaly is absent on data compiled by Cook et al. (1989). Different terrain corrections and Bouguer densities for the different datasets may be responsible for the variance. Unpublished 2.5-D gravity modeling (I. Watson and R. Lu, Exxon Production Research) indicates that variations in salt geometry produce only minor variations (<1 mgal) in the small central gravity low. Given the severity of the terrain corrections in the area, variations of this magnitude would be difficult to detect.

We therefore conclude that the geophysical anomalies are partly spurious, irrelevant, and consistent with a wide range of salt geometries that could be found with either a pinched-off diapir or meteor impact crater.

Contiguous Anticline

The low west-trending anticline adjoining the west side of Upheaval Dome (Fig. 2) supports the idea that Upheaval Dome developed as a stock growing from a deeper, elongated salt structure. The anticline could be overburden draping over a salt-cored anticline or over an uplifted basement block. Either feature would help to localize a salt diapir. Conversely, in the impact hypotheses, the juxtaposition of Upheaval Dome with an adjoining linear anticline would have to be entirely fortuitous. However, this anticline is much more subtle than Upheaval Dome, so provides only slender evidence.

Nearby Salt Structures

Undeformed Paradox Salt intersected in a nearby well (Rosen Grays Pasture #1, 27S-19E-26) is about 720 m thick. That is an ample supply of salt for diapirism. Farther away, Upheaval Dome is flanked by salt-cored anticlines (Shafer, Lockhart, Rustler, Gibson Anticlines) within 20 km to the east and by the Big Flat-Cane Creek Anticline to the north. 14 km to the east is the Meander Anticline, an upwelling of salt triggered by erosional unroofing in the Colorado canyon (Huntoon, 1982). The nearest known piercement diapir is the Moab-

Spanish Valley salt wall, 32 km to the northeast. In the Needles graben system 33 km south of Upheaval Dome, four small evaporite diapirs (Harrison, Prommel and the two Crum domes) are exposed in the lower reaches of the Colorado River's Cataract Canyon (Huntoon et al., 1982). Also here is a major gravity-glide system detaching and extending on Paradox Salt (McGill and Stromquist, 1975, 1979; Huntoon, 1982, 1988). These diverse salt structures formed in a variety of ways, but they illustrate the propensity of the Paradox Salt to deform readily in the region around Upheaval Dome.

Presence of Rim Syncline

Rim synclines typically surround salt domes and are produced by subsidence of the peripheral overburden as salt flows into the diapir. Crescentic basins within the rim syncline are also associated with salt-withdrawal (e.g., Ritz, 1936; Seni and Jackson, 1983; Jackson et al., 1990). In contrast, rim synclines are exceptionally rare in impact craters. The central uplift of an impact crater is surrounded by a flat floor or a downfaulted annular trough (Grieve and Pilkington, 1996), not a rim syncline. It could be argued that the marked rim syncline of Upheaval Dome results from a rare case of impact into an evaporite-bearing sequence. We find that implausible because Gosses Bluff impact crater (Australia), which includes a halite member below the crater, entirely lacks a rim syncline on seismic profiles (Tingate et al., 1996). Instead an almost imperceptible rim anticline is present with an overall inward dip of only 2°. Out of scores of possible impact craters described in the literature, we have found only two signs of rim synclines (others may be present, but their rarity is beyond debate). One is the BP structure, a 2.8-km-diameter circular structure in Libya that has been ascribed to impact because of shock lamellae in quartz (French et al., 1974). The other is the Sierra Madera structure in west Texas, a deeply eroded impact crater 12.5 km wide containing profuse shatter cones (Wilshire

and Howard, 1968). In neither the BP or Sierra Madera structure does the inward dip of the rim syncline (only 10° and 10–15°, respectively) approach the widespread 30° (locally >70°) inward dip of the Upheaval Dome rim syncline. .

Positive Evidence Compatible With Pinch-Off But Incompatible With Impact

Synsedimentary Structures

The most important evidence supporting diapiric pinch-off but incompatible with impact are structures indicating growth of Upheaval Dome over at least 20 m.y.: growth folds, growth faults, shifting rim synclines, onlap, truncations, and channeling. The text and illustrations describe these.

Volume Imbalance

See Part 2 (Data Repository).

Multiple Episodes of Fracturing and Cementation

Cathodoluminescence of a sample of White Rim clastic dike indicates that at least two generations of intragranular and transgranular quartz-filled microfractures formed; the filling of one fracture crosscuts another (Fig. A4a). Crosscutting fractures would be typical of any deformational event, including impact. However, the filling of the first generation fracture by authigenic quartz indicates at least two events of alternating fracturing and diagenesis. This multiple deformation is consistent with episodic faulting during protracted diapiric pinch-off but would be unlikely to form in the single instantaneous deformation event inherent in impact.

Presence of Steep Zones in Inner Limb of Rim Syncline

Instead of a peripheral flap typically rimming young impact craters, Upheaval Dome has a zone of steeply upturned strata lying 200–600 m inside the rim

syncline trace, far from the periphery. Within that zone of steepening, the Navajo dips increase abruptly inward to near-vertical or even overturned (the uncertainty in dip is due to the dominance of eolian foresets). This steep zone (Figs. 8, 11) is difficult to explain by impact because inward from here, dips decrease sharply before steepening again in the central uplift; that seems incompatible with shock zonation around a point of impact. The same argument applies to the less well-preserved steep zone in the upper Wingate-lower Kayenta.

In contrast, these steep zones have strikingly similar counterparts in salt tectonics. Poorly consolidated subsalt strata are steepened or overturned by traction exerted by the lateral flow of overlying extrusive salt. Examples of overturned subsalt flaps are known from outcrop (Jabal al Milh diapir in Yemen, Davison et al., 1996), boreholes (Wathlingen-Hänigsen diapir in Germany, Boigk, 1981; Mahogany salt sheet, Harrison and Patton, 1995), and in many proprietary seismic profiles. Based on these analogs, the steep zones enclosed by the rim syncline of Upheaval Dome record deformation beneath a radially spreading sheet of glacial salt (Fig. 23, stage 5). The extrusive salt would have deformed poorly consolidated subsalt strata by overriding them or rucking them up ahead of the glacier. The innermost zone of steep Navajo encloses a 3-km-diameter area that we envisage as formerly filled by a pancake of extrusive salt (see "Salt Tectonic Hypothesis: A Reconstruction" in the text). In the same way, the upper Wingate-lower Kayenta steep zone is thought to be the imprint of a smaller, older salt glacier against the deformation front of gravity-driven thrusting. Similar subcircular pancakes 4–15 km wide are prominent just below the seafloor in the Mississippi Canyon area of the Gulf of Mexico (e.g., Diegel et al., 1995, their Figs. 3-4).

Presence of Outward-Verging Extension

Impact craters, such as Sierra Madera (Texas) and Ries (Germany), are bounded by peripheral normal faults that dip inward. The presence of such faults at Upheaval Dome was one of the main arguments by Shoemaker and Herkenhoff (1984) for impact. However, no impact craters known to us contain equal numbers and sizes of peripheral normal faults dipping outward. That is because crater walls can only slump inward into the transient crater. In contrast, outward-dipping normal faults are common around salt domes, merely forming part of fault systems responding to downward bending of strata at the rim monocline.

Presence of Rim Monocline

A fresh impact crater has a raised rim (Shoemaker and Shoemaker, 1996). An area bounded by a radius of ~1.6 times that of the crater should be lifted above regional datum (Fig. 5a; Melosh, 1989). No such raised rim is present at Upheaval Dome. Instead, strata bend down inward below regional datum to form a peripheral rim monocline. Conversely, the rim monocline at Upheaval Dome is typical of salt diapirs having rim synclines.

Positive Evidence Compatible with Impact but Incompatible with Pinch-Off

Shatter Cones

Shatter cones typically form at low shock pressures of 2–6 GPa (Grieve and Pilkington, 1996) but locally exceeding 30–45 GPa (Stöffler, 1972). Shatter cones are nested fracture sets that curve conically about a common axis initially pointing toward the energy source of the shock (Roddy and Davis, 1977). Fractally distributed striae fan out from the apices of the conical surfaces. The cones may define the boundary between plastically deformed rock and surrounding elastically deformed rock when a compressive shock wave is

relieved by and interferes with expansion waves moving in from free surfaces of the rock (Rinehart, 1972; Roach et al., 1993). However, there is currently no satisfactory hypothesis for the formation of shatter cones (Sharpton et al., 1996).

Shatter cones are especially well developed in strong, homogeneous, fine-grained, dense rock such as carbonate but are also known in shale, sandstone, quartzite, and plutonites (Roddy and Davis, 1977). Shatter cones are prized as evidence for impact. Two “weakly developed” specimens have been reported from thin Moenkopi sandstone beds in Upheaval Dome by Kriens et al. (1997). In the same formation, they also reported the presence of roughly planar fractures having fan-shaped grooves and ridges oblique to bedding, which they termed “shatter surfaces.” No shatter cones have been reported from the numerous and thick sandstone units (Navajo, Kayenta, Wingate, Mossback) of Upheaval Dome.

Planar Microstructures in Quartz

Multiple sets of crystallographically oriented planar fractures and planar deformation features filled with diaplectic (formed in solid state) quartz glass can be generated by shock waves. These quartz microstructures were combined into four geobarometric groups by Grieve and Robertson (1976). Even the least deformed group (formed by shock pressure of 7.5 ± 3.0 GPa) has 100–250 features in 1 mm.

In contrast, according to Shoemaker and Herkenhoff (1984), “Relatively few grains with planar features or lamellae of probable shock origin” were found in the White Rim clastic dikes.” Our suite of 9 thin sections revealed no planar structures. Instead, there are abundant microfractures, many of which are only evident under cathodoluminescence (Fig. A4). The microfractures are planar or curved, and intragranular or transgranular—the latter indicating their cataclastic origin. Some of these linear microfractures are sealed by precipitation of

authigenic quartz in optical continuity around remnant fluid inclusions. The curved fractures typically radiate from points of locally high stress concentration, such as where adjoining grains impinge (Fig. A4b). These fractures, too, are filled by quartz containing tracks of fluid inclusions.

The transgranular and radiating microfractures must have formed in the dikes after or during a late stage of dike injection. These microfractures cannot be a result of brecciation by impact followed by upward transport of a slurry of crushed grains.

If genuine planar structures are actually present in the Upheaval Dome dikes, their apparent rarity could be explained by inheritance from the provenance. Alternatively, they may be merely cataclastic fractures that are abundant even in rocks that have only been buried and compacted (see previous section on "Crushed Quartz Grains").

Ejecta Breccia

During impact, an inverted conical ejecta curtain expands outward from the evacuating crater. Ejected debris falling back into the crater accumulates as a thick lens of polymict, allochthonous breccia. An ejecta blanket also spreads over the surrounding area, forming hummocks grading outward into dunes then, beyond one crater radius from the rim, into a fine-grained, patchy veneer. Kriens et al. (1997) reported the presence of a quartzose lag deposit resting on Navajo sandstone, colluvium, and wind-blown sand. They interpreted the mixture of rounded cobbles with subordinate angular fragments and broken cobbles as an impactite containing ejected bombs with nonvesicular to weakly vesicular quenched rims having little or no glass.

Salt Below Rim Syncline

In general, diapirs seem most likely to pinch-off after their source layer has been locally depleted. Grounding of surrounding overburden onto the basement (1)

restricts the supply of salt feeding the diapir, (2) disrupts the connection between diapiric salt and surrounding salt pressurized by overburden loading, and (3) removes some of the overburden load on salt through direct subsalt support of suprasalt strata.

At Upheaval Dome, the Buck Mesa well (Figs. 6, 9) indicates 450 m of salt remain below the Navajo rim syncline. For reasons that are still unclear, it appears that this diapir may have pinched off before exhausting its source layer. Alternatively, the deepest (Honaker Trail) part of the rim syncline may not directly underlie the rim syncline exposed at higher levels; the source layer could be much thinner farther outward or inward from the well. Rim-syncline positions varying with stratigraphic level are not uncommon in salt diapirs (e.g., Madirazza, 1975; Kockel, 1990).

Negative Evidence Compatible with Impact and Pinch-Off

Lack of Rock Salt at the Surface

If pinch-off had occurred, some salt residue might be present in the necked-off country rocks surrounding the vanished diapiric stem. The presence of salt would not eliminate the possibility of an origin by impact. Likewise, the absence of salt at the surface of the central uplift would not eliminate a pinched-off diapir; necking of salt is the essence of pinching off. Evaporites can also be entirely removed by dissolution even within diapirs; the Flinders diapirs (South Australia) are now devoid of halite but choked by insoluble breccia (Dalgarno and Johnson, 1968). Vast amounts of salt can be lost during salt tectonics: for example, in the Gulf of Mexico, allochthonous salt layers 6 km thick have been reduced to a salt weld of virtually zero thickness after salt was expelled laterally. Moreover, at Upheaval Dome, any traces of smeared salt at the surface would be highly vulnerable to dissolution. Some stream beds within the inner depression are

encrusted with dried salt of unknown origin, and ground water issuing from formations other than the Kayenta and Navajo is too saline to be potable (Fiero, 1958).

Lack of Nearby Piercement Diapirs

In the Paradox Basin, diapir size and maturity generally decrease away from the basin-bounding Uncompahgre Uplift. Salt bodies near the uplift tend to be diapiric walls and stocks kilometers tall. In more distal parts of the basin, where Upheaval Dome is located, most salt structures are low-relief salt anticlines and salt pillows that do not pierce their overburden. If Upheaval Dome is a pinched-off piercement salt dome, it lies more than 30 km farther outboard than any other large diapiric salt structure.

The case for Upheaval Dome's diapiric origin would be strengthened by the presence of neighboring diapirs, but their absence does not exclude the possibility of a former diapir at Upheaval Dome. The idea of a neat structural zonation in salt tectonics is an oversimplification wherever the base of the salt is faulted (as in the Paradox Basin). Isolated salt stocks are also known elsewhere (e.g., Weenzen in Germany; Green Knoll in the abyssal Gulf of Mexico).

Negative Evidence Compatible With Pinch-Off But Not With Impact

A wide variety of geologic features are spatially associated with impact craters (Fig. 5a). Most of these have not been found in other geologic settings but are also associated with nuclear-explosion craters. For that reason, natural examples of these shock-metamorphic features are generally accepted as criteria of impact (Grieve and Pilkington, 1996). Few impact craters contain all these diagnostic features, but plausible impact structures should contain at least some of them. Kriens et al. (1997) have inferred that a thickness of no more than

a few hundred meters might have been removed from the hypothetical impact crater.

Lack of Meteoritic Material

In Meteor Crater (Arizona), which is one fifth the diameter of Upheaval Dome, ~10,000 fragments of meteoritic Fe-Cr-Ni have been recovered and meteoritic dust is present up to 10 km from the impact (Hodge, 1994). In contrast, no meteoritic particles, even preserved as veinlets in microfractures, have been reported from Upheaval Dome. Nor has enrichment in siderophile elements due to meteoritic admixture.

Lack of Melt

Shock, viscous flow, and friction melt target rocks during impact. The melts mix with breccia, pools, and veins in the base and sides of a crater below the breccias deposited by fallback and debris sliding. Melt also occurs at higher stratigraphic levels as vapor spherules, liquid bombs and fragments mixed with other ejecta (Masaitis, 1994). Melting at moderately low shock pressure is enhanced by porous sedimentary rocks like sandstone (Grieve and Pilkington, 1996). Yet no melts have been found at Upheaval Dome, though Kriens et al. (1997) have interpreted recrystallized quenched rims in quartzose cobbles.

Lack of In-Situ Breccia

The floor of an impact crater compresses by the shock wave then decompresses by rarefaction. That expansion shatters the rock in situ, forming a thick lens of para-autochthonous monomict breccia below the central mound (Fig. 5a). In addition, breccia dikes extend out to the rim of the target rocks (Grieve and Pilkington, 1996). No in-situ breccia units have been reported from Upheaval Dome.

Lack of Shock-Metamorphic Minerals

Shocked rocks contain selective phase transitions in which ultra-high-pressure mineral phases are juxtaposed against phases formed under much lower pressures. Diaplectic glass of quartz or feldspar, and coesite and stishovite (dense shock-metamorphic phases of quartz) should be abundant in the numerous sandstone units of Upheaval Dome, but no traces have been reported.

Lack of Outer Fault Terracing

Large terrestrial craters become gravitationally modified by inward slumping of the walls of the transient crater. The annular normal faults create terraced, outward-dipping strata on margin of crater (Fig. 5a). In contrast, stratal dip is invariably inward at the rim monocline on the periphery of Upheaval Dome.

Lack of Overturned Peripheral Flap

Overturned strata forming flaps characterize the outer rim of craters produced by especially high-energy impacts (Fig. 5a; Shoemaker, 1960). The absence of such a flap at Upheaval Dome could be explained by low-energy impact or by deep erosion.

REFERENCES CITED

- Anders, M. H., and Wiltschko, D. V., 1994, Microfracturing, paleostress and the growth of faults: *Journal of Structural Geology*, v. 16, p. 795–815.
- Boigk, H., 1981, *Erdöl und Erdölgas in der Bundesrepublik Deutschland*: Stuttgart, Springer-Verlag, 328 p.
- Collinson, J. D., 1994, Sedimentary deformational structures, in Maltman, A., ed., *The geological deformation of sediments*: New York, Chapman & Hall, p. 95-125.

Cook, K. L., Bankey, V., Mabey, D. R., and DePangher, M., 1989, Complete

Bouguer gravity anomaly map of Utah: Utah Geological and Mineral Survey
Map 122.

Dalgarno, C. R., and Johnson, J. E., 1968, Diapiric structures and late
Precambrian-early Cambrian sedimentation in Flinders Ranges, South
Australia, *in* J. Braunstein and G. D. O'Brien (eds.), Diapirism and diapirs—
a symposium: American Association of Petroleum Geologists Memoir 8, p.
301–314.

Davison, I., Bosence, D., Alsop, G. I., and Al-Aawah, M. H., 1996, Deformation
and sedimentation around active Miocene salt diapirs on the Tihama Plain,
northwest Yemen, *in* Alsop, G. I., Blundell, D. J., and Davison, I., eds., Salt
tectonics: Geological Society, London, Special Publication No. 100, p. 23-
39.

Dickinson, W. W., and Milliken, K. L., 1995, The diagenetic role of brittle
deformation in compaction and pressure solution, Etjo Sandstone, Namibia:
Journal of Geology, v. 103, p. 339–347.

French, B. M., 1974, Shock-metamorphic features in two meteorite impact
structures, Southeastern Libya: *Geological Society of America Bulletin*, v.
85, p. 1425-1428.

Grieve, R. A. F., and Robertson, P. B., 1976, Variation in shock deformation at
the Slate Islands impact structure, Lake Superior: *Contributions to
Mineralogy and Petrology*, v. 58, no. 1, p. 37-51.

Grieve, R. A. F., and Pilkington, M., 1996, The signature of terrestrial impacts:
AGSO Journal of Australian Geology and Geophysics, v. 16, p. 399–420.

Haines, P. W., 1996, Goyder impact structure, Arnhem Land, Northern Territory:
AGSO Journal of Australian Geology and Geophysics, v. 16, p. 561–566.

- Harrison, H., and Patton, B., 1995, Translation of salt sheets by basal shear, in Travis, C. J., Harrison, H., Hudec, M. R., Vendeville, B. C., Peel, F. J., and Perkins, B. F., eds., Salt, sediment and hydrocarbons: Gulf Coast Section of Society of Economic Paleontologists and Mineralogists Foundation Sixteenth Annual Research Conference, Houston, p. 99-107.
- Hodge, P., 1994, Meteorite craters and impact structures of the Earth: New York, Cambridge University Press, 124 p.
- Huntoon, P. W., 1982, The Meander anticline, Canyonlands, Utah: an unloading structure resulting from horizontal gliding on salt: Geological Society of America Bulletin, v. 93, p. 941-950.
- Jackson, M. P. A., 1982, Fault tectonics of the East Texas Basin: Bureau of Economic Geology Geological Circular 82-84, The University of Texas at Austin, 31p.
- Jackson, M. P. A., and Cramez, C., 1989, Seismic recognition of salt welds in salt tectonics regimes, *in* Gulf of Mexico salt tectonics, associated processes and exploration potential: Gulf Coast Section of the Society for Economic Paleontologists and Mineralogists Foundation Tenth Annual Research Conference Program and Extended and Illustrated Abstracts, p. 66-71.
- Joesting, H. R., and Plouff, D., 1958, Geophysical studies of the Upheaval Dome area, San Juan County, Utah: Intermountain Association of Petroleum Geologists, Ninth Annual Field Conference, Paradox Basin, p. 86-92.
- Kockel, F., 1990, Morphology and genesis of Northwest-German salt structures, *in* Proceedings, Symposium on diapirism with special reference to Iran, vol. 1, Islamic Republic: Iran, Tehran University Governory of Hormozgan, Ministry of Mines and Metals, p. 225-245.

- Madirazza, I., 1975, The geology of the Vejrum salt structure, Denmark:
Geological Society of Denmark Bulletin, vol. 24, p. 161-171.
- Masaitis, V. L., 1994, Impactites from Popigai crater, in Dressler, B. O., Grieve,
R. A. F., and Sharpton, V. L., eds., Large meteorite impacts and planetary
evolution: Boulder, Colorado, Geological Society of America Special Paper
293, p. 153-162.
- McGill, G. E. and A. W. Stromquist, 1975, Origin of graben in the Needles
District, Canyonlands National Park, Utah: Four Corners Geological society
Guidebook, 8th Field Conference, Canyonlands, p. 235-243.
- McGill, G. E. and A. W. Stromquist, 1979, The Grabens of Canyonlands National
Park, Utah: geometry, mechanics, and kinematics: Journal of Geophysical
Research, v. 84, no. B9, p. 4547-4563.
- Melosh, H. J., 1989, Impact cratering a geologic process: New York, Oxford
University Press, 245 p.
- Milliken, K. L., 1994, The widespread occurrence of healed microfractures in
siliciclastic rocks: Evidence from scanned cathodoluminescence imaging, *in*
Nelson, P. P., and Laubach, S. E., eds., Rock mechanics: Models and
measurements, challenges from industry: Rotterdam, A. A. Balkema, p.
825-832.
- Milton, D. J., Glikson, A. Y., and Brett, R., 1996, Gosses Bluff—a latest Jurassic
impact structure, central Australia. Part 1: geological structure, stratigraphy,
and origin: AGSO Journal of Australian Geology and Geophysics, v. 16, p.
453–486.
- Milton, L. W., 1987, The Hico impact structure of North-Central Texas in Pohl, J.,
ed., Research in terrestrial impact structures: Braunschweig, Wiesbaden,
Friedr. Vieweg & Sohn, p. 131-140.

- Puffett, W. P., Weir G. W., and Dodson C. L., 1957, Collapse structures in Spanish Valley, San Juan and Grand Counties, Utah: Geological Society of America Bulletin, v. 68, p. 1842.
- Rinehart, J. S., 1972, Some experimental data relating to the mechanics of shatter cone formation [abs.]: EOS (Transactions, American Geophysical Union), v. 53, no. 4, p. 427.
- Roach, D. E., Fowler, A. D., and Fyson, W. K., 1993, Fractal fingerprinting of joint and shatter-cone surfaces: *Geology*, v. 21, p. 759-762.
- Roddy, D. J., and Davis, K. L., 1977, Shatter cones formed in large-scale experimental explosion craters, in Roddy, D. J., Pepin R. O., Merrill, R. B., eds., *Impact and explosion cratering*: New York, Pergamon Press, p. 715-750.
- Sharpton, V. L., Dressler, B. O., Herrick, R. R., Schneiders, B., and Scott, J., 1996, New constraints on the State Islands impact structure, Ontario, Canada: *Geology*, v. 24, p. 851–854.
- Shoemaker, E. M., 1960, Penetration mechanics of high velocity meteorites, illustrated by meteor crater, Arizona: International Geological Congress, 21st, Copenhagen, Proc. Sec. 18, p. 418-434.
- Shoemaker, E. M., and Shoemaker, C. S., 1996, The Proterozoic impact record of Australia: *AGSO Journal of Australian Geology and Geophysics*, v. 16, p. 379–398.
- Stöffler, D., 1972, Deformation and transformation of rock-forming minerals by natural and experimental shock pressures: *Fortschritte der Mineralogie*, v. 49, p. 50–113.
- Tingate, P. R., Lindsay, J. F., and Marshallsea, S. J., 1996, Impact structures as potential petroleum exploration targets: Gosses Bluff, a Late Jurassic

example in central Australia: AGSO Journal of Australian Geology and Geophysics, v. 16, p. 529–552.

Wilshire, H. G., and Howard, K. A., 1968, Structural pattern in central uplifts of cryptoexplosion structures as typified by Sierra Madera: *Science*, v. 162, p. 258-261.

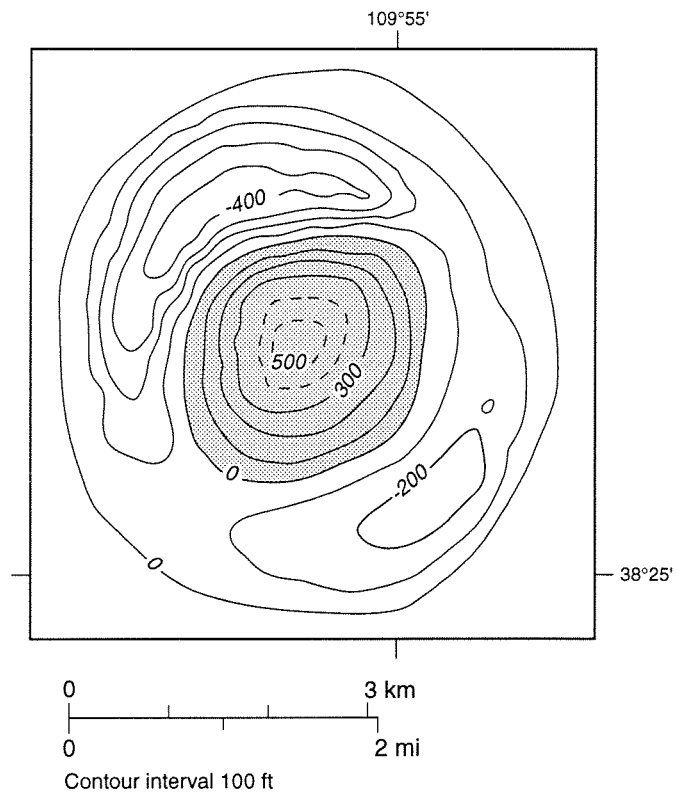
FIGURE CAPTIONS

Figure A4. Microfractured quartz in the White Rim clastic dikes from the core of Upheaval Dome. All the features illustrated, which were produced by mechanical rearrangement under brittle conditions, are typical of sandstones undergoing only burial and are especially common near faults. (a) Image obtained by electron-beam-induced cathodoluminescence showing a grain containing two generations of microfractures separated by an episode of fracture sealing by optically continuous, less luminescent, authigenic quartz (image by Rob Reed). Scale bar is 100 μm long. (b) Photomicrographs of linear microfractures, filled by authigenic quartz, which radiate from the high-stress area where adjoining grains impinge (image by Steve Laubach). The short axis of the fractured grain is about 100 μm wide.

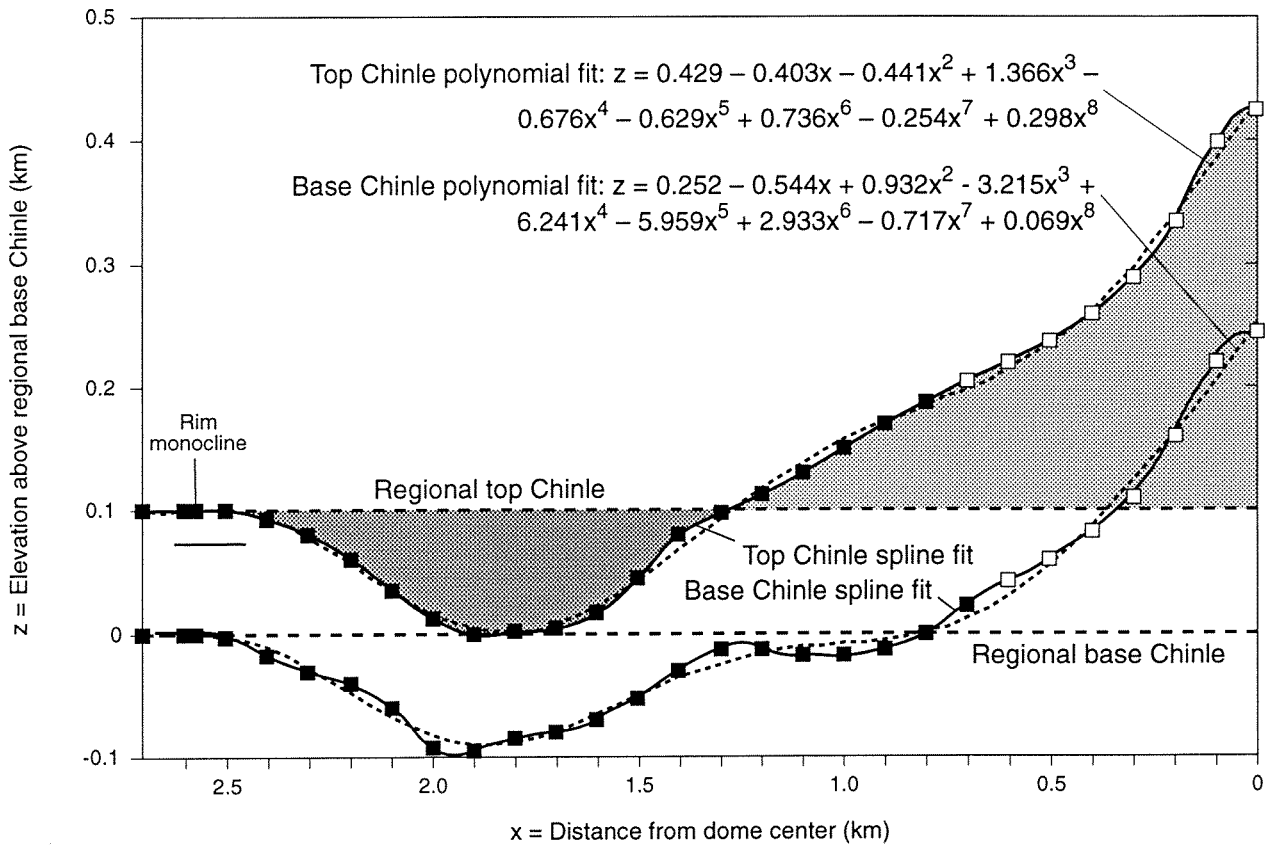
Figure A5. Air photograph of Dome 16 in the Great Kavir salt desert of Central Iran. This erosional section through the Tertiary diapir shows variegated evaporitic playa-lacustrine strata that have been folded increasingly inward to a core of marine salt. The comparative geometry of the two main evaporite units indicates that the stem of this diapir is almost pinched off (see Jackson et al., 1990, for details). We equate these radial folds with those in the core of Upheaval Dome. The periphery of Dome 16 is an upturned collar of strongly sheared country rock that passes outward into gently curved strata responding to regional folding in the Elburz foreland.

Scattered playas slightly obscure the underlying structure. The diapir is 5.0

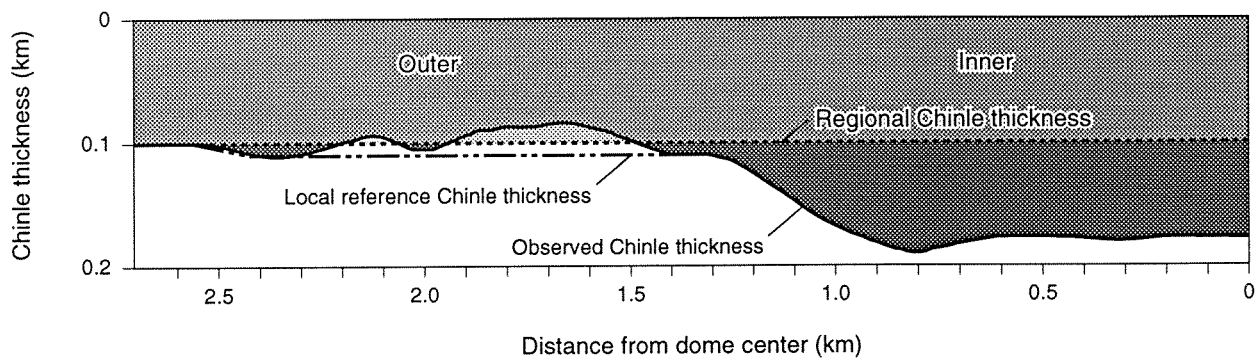
∞ 2.7 km in size.



(a)



(b)



Reference state

Present state

Case 1 = RT + outer primary thinning/thickening + inner primary thickening



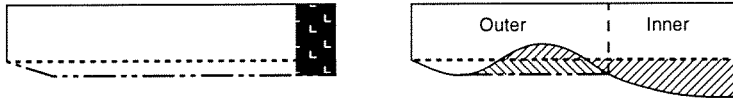
Case 2 = LRT + diapir + outer structural thinning + inner primary thickening



Case 3 = LRT + diapir + outer primary thickening/structural thinning + inner primary thickening



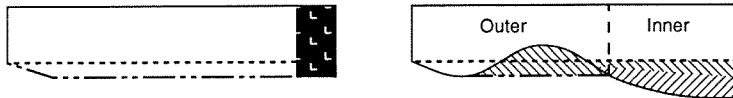
Case 4 = LRT + diapir + outer primary/structural thinning + inner primary thickening


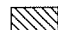



Case 5 = RT + diapir + outer structural thinning/thickening + inner primary thickening



Case 6 = LRT + diapir + outer structural thinning + inner primary/structural thickening



 Primary thickness change
 Structural thickness change
 Former diapir

- - - - - Regional thickness (RT)
 - - - - - Local reference thickness (LRT)

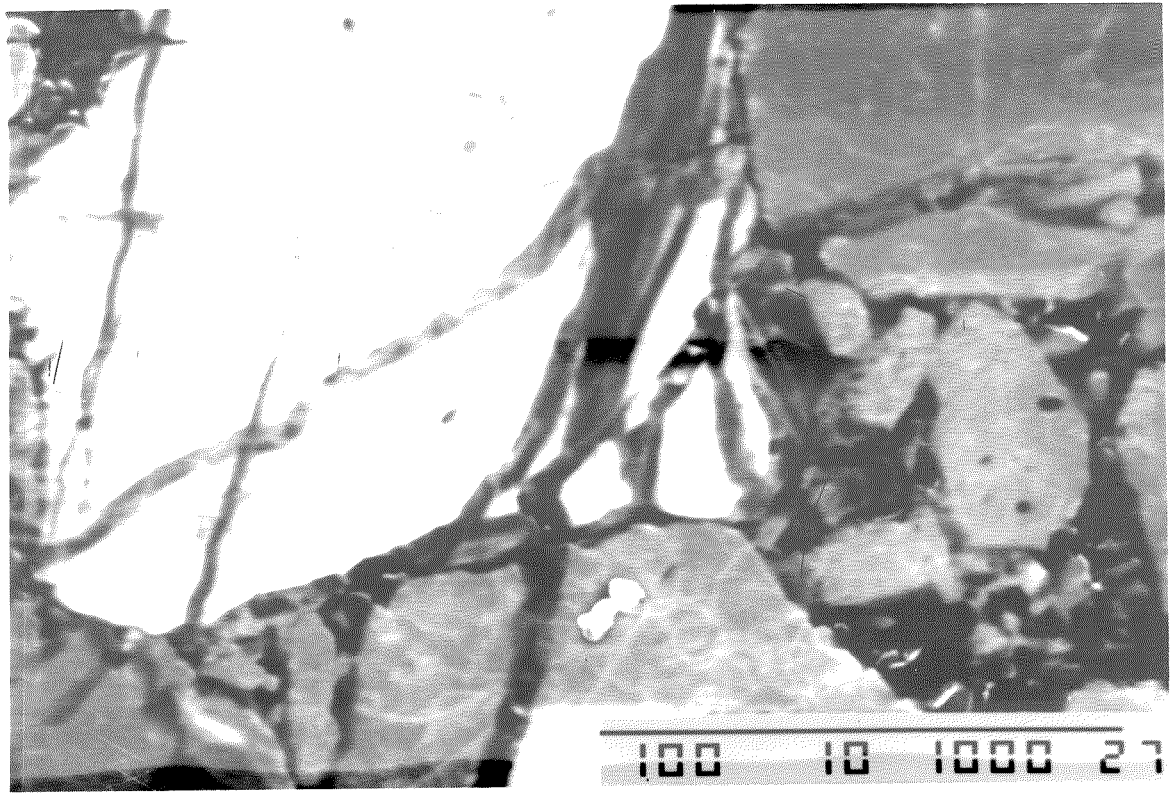


Fig. A4-A

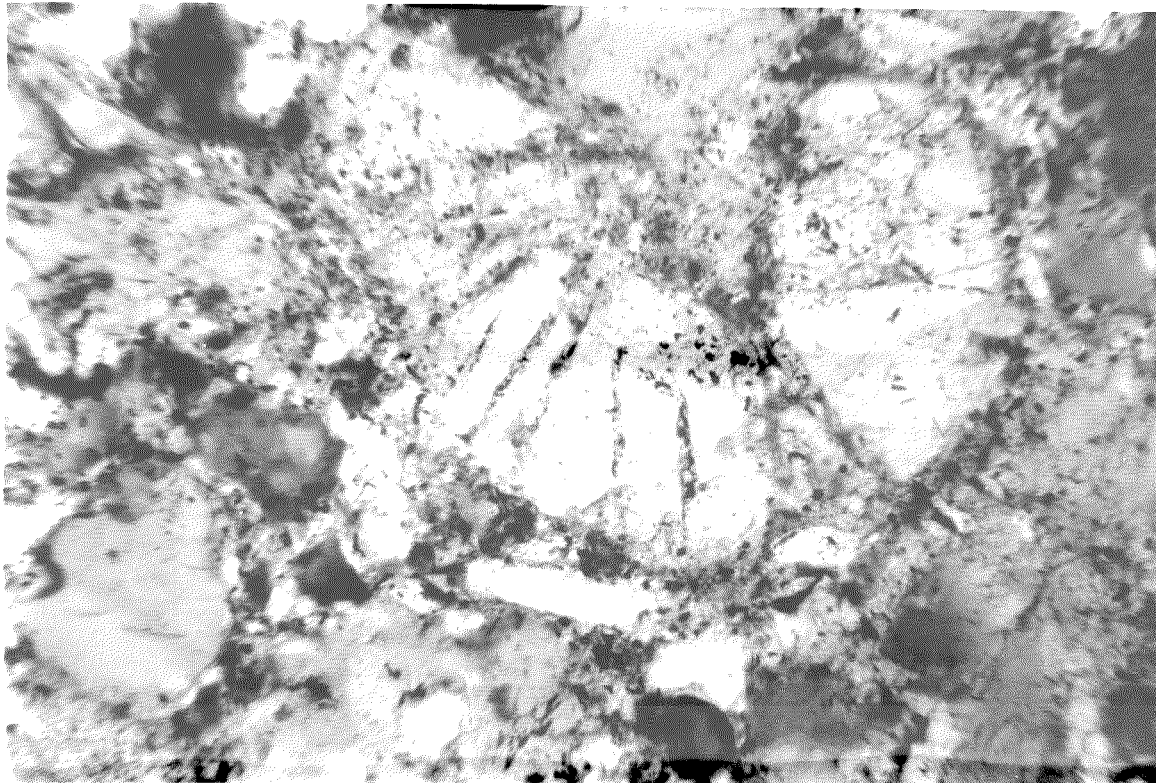


Fig. A 4-B

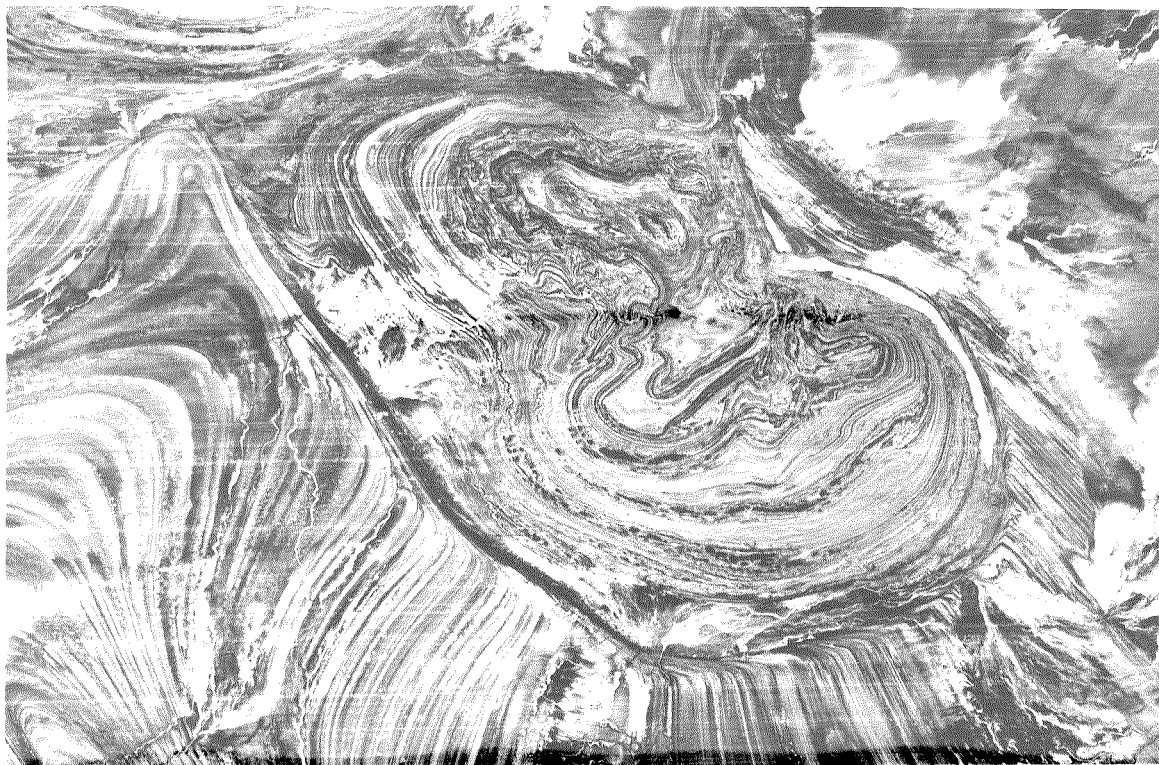


Fig. A S